

Current in molecular junctions: Effects of system-reservoir coupling

Hari Kumar Yadalam and Upendra Harbola

Inorganic and Physical Chemistry, Indian Institute of Science, Karnataka, India.

We study the effect of system reservoir coupling strength on the current flowing through quantum junctions. We consider two simple double quantum dot configurations coupled to two external fermionic reservoirs and calculate the net current flowing between the two reservoirs. The net current is partitioned into currents carried by the eigenstates of the system and by the coherences induced between the states due to coupling with the leads. We find that current carried by populations is always positive whereas current carried by coherences may be negative. This results in a non-monotonic dependence of the net current on the coupling strength. We find that in certain cases, the net current can vanish at large couplings due to cancellation between currents carried by the states and the coherences. These results provide new insights into the non-trivial role of system-reservoir couplings on electron transport through quantum dot junctions.

I. INTRODUCTION

Transport properties of quantum junctions have been studied for over two decades motivated not only by their technological relevance but also the opportunities they provide to explore fundamental physics. For example quantum dot junctions provide a good platform for verification of fundamental concepts, like fluctuation theorems [1, 2]. There have also been a lot of technologically relevant proposals of diodes [3], transistors [4], heat engines [5, 6], which can be realized using quantum junctions made of single molecules or quantum dots. Quantum dot junctions can also serve as promising candidates for realizing quantum computers [7].

Current flowing through quantum dot junctions have been measured experimentally [8] and studied using various theoretical formulations like quantum master equations (QME) [9], scattering matrix (SM) [10], and non equilibrium Green's function (NEGF) method [11]. QME and SM approaches are valid within a certain parameter regime, but NEGF method is exact and can be applied in all regimes, although analytically tractable results can be obtained only for non-interacting systems.

Although a good amount of theoretical work on quantum conduction exists in the literature, however the role of system-reservoir coupling has not been much emphasized, except in the discussions of decoherence [12]. How does the current vary as system-reservoir coupling is changed? To answer this question we note that, in a simple scattering picture, the system-reservoir coupling offers resistance to the tunneling electrons. Higher the coupling, lower the resistance and, therefore, larger is the current. This picture is in full agreement with the results of quantum master equation formulation which predicts a monotonic increase in the current as the coupling is increased. However, this does not present the complete picture and it is not at all obvious what happens as one goes beyond the regime of QME or simple scattering picture.

In this work we explore the effect of strong system-reservoir couplings on the net current flowing through quantum junctions. We find that current is not always

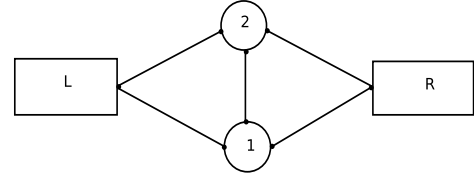


FIG. 1. Schematic of model system considered. It consists of two localized sites coupled to two fermionic reservoirs.

an increasing function of the coupling strength. In fact, surprisingly, we find that for certain cases, the net current may diminish at large coupling strengths. As we discuss below, this surprising behavior is a consequence of the quantum interference between the eigenstates which carries a negative (against the applied bias) current which may cancel the current contributions coming from the eigenstates. The current behavior for large couplings, of course, depends on the quantum dot configuration and is not universal. For certain configurations, there is an optimal value of the coupling strength at which the current is maximal.

To explore this current behavior we consider two simple models both consist of two quantum dots coupled to two fermionic reservoirs but differ in their configurations. This is discussed in the next section. In Sec. (III), we calculate the net current flowing through these junctions and partition it into contributions coming from populations and coherences and analyze the behavior of these contributions as a function of system reservoir coupling strengths. We present conclusions in Sec. (IV).

II. MODEL HAMILTONIAN AND CURRENT CALCULATION

We start by considering a simple model shown in Fig. 1. It consists of two quantum dots each having a single electron orbital coupled to each other and also coupled to two fermionic reservoirs.

The Hamiltonian describing this model is given as,

$$\begin{aligned} \hat{H} = & \sum_{i,j=1}^2 H_{0ij} c_i^\dagger c_j + \sum_{\alpha=L,R} \sum_k \epsilon_{\alpha,k} d_{\alpha k}^\dagger d_{\alpha k} \\ & + \sum_k \left[g_L^{(1)} d_{Lk}^\dagger c_1 + g_R^{(1)} d_{Rk}^\dagger c_1 + g_L^{(2)} d_{Lk}^\dagger c_2 \right. \\ & \left. + g_R^{(2)} d_{Rk}^\dagger c_2 + h.c. \right] \end{aligned} \quad (1)$$

where

$$H_0 = \begin{pmatrix} \epsilon_1 & -t \\ -t & \epsilon_2 \end{pmatrix} \quad (2)$$

is the single particle Hamiltonian for the isolated molecule. Here c_i (c_i^\dagger) are the fermionic annihilation (creation) operators for destroying (creating) electron at site 'i' and similarly $d_{\alpha k}$ ($d_{\alpha k}^\dagger$) are operators for destroying (creating) electron in state labeled by 'k' in the ' α ' lead ($\alpha = L/R$). First two terms in the Hamiltonian represent isolated system and lead Hamiltonians, and the third term represents hybridization between system and lead sites with $g_\alpha^{(1)}$ and $g_\alpha^{(2)}$ representing coupling of the α th lead with dot (1) and dot (2), respectively. We have also assumed wide-band approximation (system lead coupling is independent of 'k').

The net current I_L (same as $-I_R$) flowing into the left lead at steady-state is given by the rate of change of charge on the left lead i.e., $I_L(t) = \frac{d}{dt}(-e \sum_k d_{LK}^\dagger d_{LK})$. The net current can be expressed in terms of system greater and lesser Green's functions [11, 13] $G^{>/<}$ as,

$$I_L = \frac{e}{\hbar} \int_{-\infty}^{+\infty} \frac{d\omega}{2\pi} Tr [\Sigma_L^<(\omega) G^>(\omega) - G^<(\omega) \Sigma_L^>(\omega)], \quad (3)$$

where $\Sigma_L^{>/<}$ and $G^{>/<}$ are Fourier transformed greater and lesser projections of contour ordered self-energy due to left lead and the system Greens' functions introduced below.

Green's functions (in matrix form) are defined on Schwinger-Keldysh contour [14] as,

$$\begin{aligned} G^c(\tau, \tau') = & -\frac{i}{\hbar} \langle [\Theta(\tau, \tau') \Psi(\tau) \Psi^\dagger(\tau') - \Theta(\tau', \tau) \Psi^\dagger(\tau')^T \Psi(\tau)^T] \rangle \end{aligned} \quad (4)$$

where τ and τ' are contour times with, $\Psi(\tau) = (c_1(\tau), c_2(\tau))$ and $\Theta(\tau, \tau')$ is the Heaviside step function defined on the Schwinger-Keldysh contour. $G^c(\tau, \tau')$ satisfies the following equation of motion

$$\int_c d\tau_1 \left[(i\hbar \frac{\partial}{\partial \tau} - H_S) \delta^c(\tau, \tau_1) - \Sigma^c(\tau, \tau_1) \right] G^c(\tau_1, \tau') = \delta^c(\tau, \tau')$$

where Σ^c is the self-energy due to interaction with the leads and it is given as sum of self energies due to left

and right leads i.e., $\Sigma^c(\tau, \tau') = \sum_{\alpha=L,R} \Sigma_\alpha^c(\tau, \tau')$. The self energies due to leads is given by a 2×2 matrix with element (i, j) defined as,

$$[\Sigma_\alpha^c(\tau, \tau')]_{ij} = g_\alpha^{(i)*} g_\alpha^{(j)} \sum_{k,k'} G_{\alpha k, \alpha k'}^0(\tau, \tau') \quad (6)$$

Here $G_{Lk, Lk'}^0(\tau, \tau')$ and $G_{Rk, Rk'}^0(\tau, \tau')$ are contour ordered Green's functions for the isolated leads. Equation (5) can be projected onto the real times using Langreth rules to obtain all other real-time Green's functions. At steady-state all the Green's functions become time translation invariant and can be handled easily in the frequency domain. Thus obtained Green's functions can be used in Eq. (3) to get expression for the net current, I_L [11, 15].

For simplicity we consider two cases : serial couple dot system (obtained in the limit $g_L^{(2)} = g_R^{(1)} = 0$) and side coupled dot system (obtained in the limit $g_L^{(2)} = g_R^{(2)} = 0$). We further assume all couplings between sites are equal in strength and site energies are same as the Fermi energy of the two leads (set to zero).

The net current for serially coupled dot system is obtained as (we use units such that $e = 1$, $c = 1$ and $\hbar = 1$)

$$I_L = \int_{-\infty}^{+\infty} d\omega \left[\frac{\Gamma^2 t^2}{(\omega^2 - t^2 - (\frac{\Gamma}{2})^2)^2 + \omega^2 \Gamma^2} \right] [f_L(\omega) - f_R(\omega)]. \quad (7)$$

For the side coupled dot system, the net current is

$$I_L = \int_{-\infty}^{+\infty} d\omega \left[\frac{\Gamma^2 \omega^2}{(\omega^2 - t^2)^2 + \omega^2 \Gamma^2} \right] [f_L(\omega) - f_R(\omega)]. \quad (8)$$

Here $f_\alpha(\omega) = \frac{1}{e^{\beta_\alpha(\omega - \mu_\alpha)} + 1}$ is the Fermi function of two leads ($\alpha = 1, 2$), β_α and μ_α are, respectively, the temperature and the chemical potential of α^{th} lead.

These currents are plotted against Γ in fig. (2) for $t = 1$, $\mu_L = 1$, $\mu_R = -1$ and $\beta_L^{-1} = \beta_R^{-1} = 0$. It is clear that net current is not always an increasing function of Γ . For side coupled dot system, net current is an increasing function of Γ and saturates asymptotically to a constant value for large Γ , which for zero temperature is simply proportional to the difference in chemical potentials of the two leads. However, for serial coupled dot system, the net current shows a non-monotonic behavior and settles to zero for large Γ . The latter case is very counter intuitive and, in order to understand these two completely different current behaviors, below we analyze currents in the eigenbasis of the system.

III. PARTITIONING THE CURRENT

- (5) We define a unitary transformation matrix, \mathcal{U} , which diagonalizes the system Hamiltonian H_0 i.e., $\mathcal{U} = \frac{1}{\sqrt{2}} \begin{pmatrix} 1 & 1 \\ 1 & -1 \end{pmatrix}$. We next transform the system lesser and

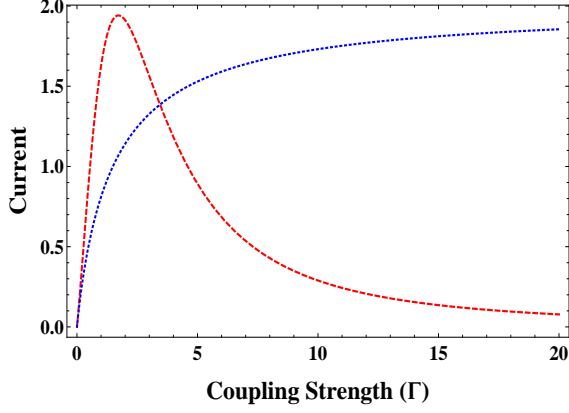


FIG. 2. (Color online) Net current as a function of Γ for serial coupled (red-dashed-thick) and side coupled (blue-dotted-thin) systems. Here $t = 1$, $\beta_L^{-1} = \beta_R^{-1} = 0$, $\mu_L = 1$ and $\mu_R = -1$.

greater Green's functions $G^{</>}(\omega)$ and lesser and greater left-lead self-energies $\Sigma_L^{</>}(\omega)$ into the eigenbasis using, $A \rightarrow \bar{A} = U^\dagger A U$, where A is any matrix defined in the local basis. Thus transforming Eq. (3) to eigenbasis, the net current can be partitioned into currents carried by the population in the bonding state (I_b), population in the anti-bonding state (I_a), and the current carried by coherences (I_c). The expressions for which are given as

$$I_b = \int_{-\infty}^{+\infty} d\omega [\Sigma_{Lbb}^{<}(\omega) G_{bb}^{>}(\omega) - G_{bb}^{<}(\omega) \Sigma_{Lbb}^{>}(\omega)], \quad (9)$$

$$I_a = \int_{-\infty}^{+\infty} d\omega [\Sigma_{La a}^{<}(\omega) G_{aa}^{>}(\omega) - G_{aa}^{<}(\omega) \Sigma_{La a}^{>}(\omega)] \quad (10)$$

and

$$I_c = \int_{-\infty}^{+\infty} d\omega [\Sigma_{Lba}^{<}(\omega) G_{ab}^{>}(\omega) - G_{ab}^{<}(\omega) \Sigma_{Lba}^{>}(\omega) + \Sigma_{Lab}^{<}(\omega) G_{ba}^{>}(\omega) - G_{ba}^{<}(\omega) \Sigma_{Lab}^{>}(\omega)]. \quad (11)$$

We next specialize to two simple models introduced in the previous section to gain a better insights into the role of system reservoir coupling strength on current.

Serially coupled system

For the serially coupled double quantum dot system case the explicit expressions for I_b , I_a and I_c are

$$I_b = \int_{-\infty}^{+\infty} d\omega \left[\frac{(\frac{\Gamma}{2})^2}{(\omega + t)^2 + (\frac{\Gamma}{2})^2} \right] [f_L(\omega) - f_R(\omega)], \quad (12)$$

$$I_a = \int_{-\infty}^{+\infty} d\omega \left[\frac{(\frac{\Gamma}{2})^2}{(\omega - t)^2 + (\frac{\Gamma}{2})^2} \right] [f_L(\omega) - f_R(\omega)] \quad (13)$$

and

$$I_c = \int_{-\infty}^{+\infty} d\omega \left[\frac{-2(\frac{\Gamma}{2})^2 (\omega^2 - t^2 + (\frac{\Gamma}{2})^2)}{(\omega^2 - t^2 - (\frac{\Gamma}{2})^2)^2 + \omega^2 \Gamma^2} \right] [f_L(\omega) - f_R(\omega)]. \quad (14)$$

Here we treat the lead induced self-energies within the wide-band approximation and assume that the left lead and quantum dot (1) coupling strength is the same as the right lead and quantum dot (2) coupling, that is, $\Gamma_L = \Gamma_R = \Gamma$. The above integrals can be easily done for zero temperature case ($\beta_L^{-1} = \beta_R^{-1} = 0$) to get

$$I_b = \frac{\Gamma}{2} \left[\tan^{-1}\left(\frac{V+2t}{\Gamma}\right) + \tan^{-1}\left(\frac{V-2t}{\Gamma}\right) \right] \quad (15)$$

and $I_a = I_b$ at zero temperature for the symmetrically biased system ($\mu_L = \frac{V}{2}$ and $\mu_R = -\frac{V}{2}$). The coherent contribution is obtained as

$$I_c = \left(\frac{\Gamma^2}{4t^2 + \Gamma^2} \right) \left\{ t \log \left(\frac{(V+2t)^2 + \Gamma^2}{(V-2t)^2 + \Gamma^2} \right) - \Gamma \left[\tan^{-1}\left(\frac{V+2t}{\Gamma}\right) + \tan^{-1}\left(\frac{V-2t}{\Gamma}\right) \right] \right\} \quad (16)$$

The expressions for current contributions from the bond-

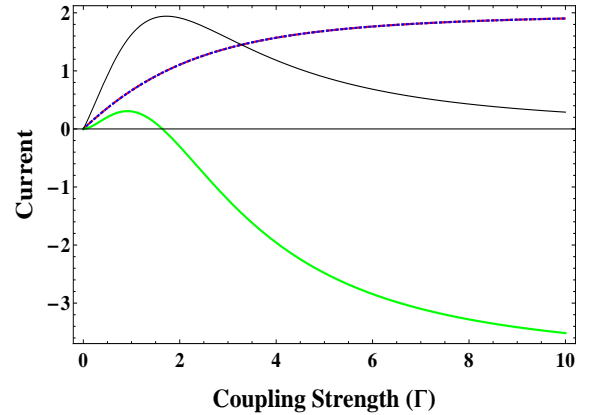


FIG. 3. (Color online) Currents carried by bonding (red-dashed), anti-bonding (blue-dotted) and coherences (green-thick) along with the net current (black-thin) as a function of Γ with $t = 1$, $\beta_L^{-1} = \beta_R^{-1} = 0$, $\mu_L = 1$ and $\mu_R = -1$.

ing and the anti-bonding orbitals are identical to the one obtained for a single resonant level with energies $-t$ and t , respectively. These contributions are always positive (throughout, we assume $\mu_L > \mu_R$ and the two leads have the same temperature). However, as noted from Eq. (14) or (16), the coherent contribution can be positive or negative depending on the relative values of the coupling strengths Γ and t . For large Γ , coherent contribution is always negative which can compete with the contributions from the populations. Current contributions from eigenstate populations and coherences and the net current are plotted as a function of Γ in fig. (3). Here

bonding and anti-bonding (population) contributions are equal due to the parameters chosen ($\epsilon_1 = \epsilon_2 = 0$ and $\mu_R = -\mu_L$). These contributions increase with Γ and saturate to a non zero constant value for large Γ , which corresponds to unit conductance (e^2/h) per electron channel. The coherent contribution shows non monotonic trend, initially increases but finally settles down to a negative value which is the sum of bonding and anti-bonding contributions for large Γ . This non-monotonic character in I_c is seen only for bias values $V \leq 2t$. For large values of the bias $V \gg 2t$, the coherent contribution is always negative. Thus for intermediate bias values, it should be possible to maximize the net current by suitably choosing the coupling strength. For $V \ll 2t$, the coherent contribution vanishes if $\Gamma = 2t$ and the net current is maximum.

For large Γ , the conductivity of the two population channels (bonding and anti-bonding states) is unity while that of the coherent channel approaches to 2, although in the opposite direction to the applied bias. Thus for large Γ , both population channels and coherence channel conduct equal current but in the opposite directions, which leads to a vanishing net current for large Γ .

Side coupled system

Next we consider the case when $g_L^{(2)} = g_R^{(2)} = 0$. In this case the explicit expressions for I_b , I_a and I_c are obtained as follows.

$$I_b = \frac{1}{4} \int_{-\infty}^{+\infty} d\omega \left[\frac{\Gamma^2(\omega - t)^2}{(\omega^2 - t^2)^2 + \omega^2 \Gamma^2} \right] [f_L(\omega) - f_R(\omega)], \quad (17)$$

$$I_a = \frac{1}{4} \int_{-\infty}^{+\infty} d\omega \left[\frac{\Gamma^2(\omega + t)^2}{(\omega^2 - t^2)^2 + \omega^2 \Gamma^2} \right] [f_L(\omega) - f_R(\omega)] \quad (18)$$

and

$$I_c = \frac{1}{2} \int_{-\infty}^{+\infty} d\omega \left[\frac{\Gamma^2(\omega^2 - t^2)}{(\omega^2 - t^2)^2 + \omega^2 \Gamma^2} \right] [f_L(\omega) - f_R(\omega)]. \quad (19)$$

Here again we have assumed that left and right leads are coupled to quantum dot 2 with equal strength ($\Gamma_L = \Gamma_R = \Gamma$). The analytic expressions for these currents for

zero temperature case are obtained as follows.

$$I_b = \left(\frac{\Gamma}{2}\right)^2 \left\{ \frac{(a_1 - t)^2}{(a_1 - a_2)(a_1 - a_3)(a_1 - a_4)} \log\left(\frac{a_1 - \frac{V}{2}}{a_1 + \frac{V}{2}}\right) + \frac{(a_2 - t)^2}{(a_2 - a_1)(a_2 - a_3)(a_2 - a_4)} \log\left(\frac{a_2 - \frac{V}{2}}{a_2 + \frac{V}{2}}\right) + \frac{(a_3 - t)^2}{(a_3 - a_1)(a_3 - a_2)(a_3 - a_4)} \log\left(\frac{a_3 - \frac{V}{2}}{a_3 + \frac{V}{2}}\right) + \frac{(a_4 - t)^2}{(a_4 - a_1)(a_4 - a_2)(a_4 - a_3)} \log\left(\frac{a_4 - \frac{V}{2}}{a_4 + \frac{V}{2}}\right) \right\}. \quad (20)$$

I_a is obtained by replacing t with $-t$ in Eq. (20), and

$$I_c = \left(\frac{\Gamma}{2}\right)^2 \left\{ \frac{1}{(a_1 - a_2)} \left[\log\left(\frac{a_1 - \frac{V}{2}}{a_1 + \frac{V}{2}}\right) - \log\left(\frac{a_2 - \frac{V}{2}}{a_2 + \frac{V}{2}}\right) \right] + \frac{1}{(a_3 - a_4)} \left[\log\left(\frac{a_3 - \frac{V}{2}}{a_3 + \frac{V}{2}}\right) - \log\left(\frac{a_4 - \frac{V}{2}}{a_4 + \frac{V}{2}}\right) \right] \right\} \quad (21)$$

where $a_1 = -i\frac{\Gamma}{2} + \sqrt{t^2 - (\frac{\Gamma}{2})^2}$, $a_2 = -i\frac{\Gamma}{2} - \sqrt{t^2 - (\frac{\Gamma}{2})^2}$, $a_3 = i\frac{\Gamma}{2} + \sqrt{t^2 - (\frac{\Gamma}{2})^2}$ and $a_4 = i\frac{\Gamma}{2} - \sqrt{t^2 - (\frac{\Gamma}{2})^2}$.

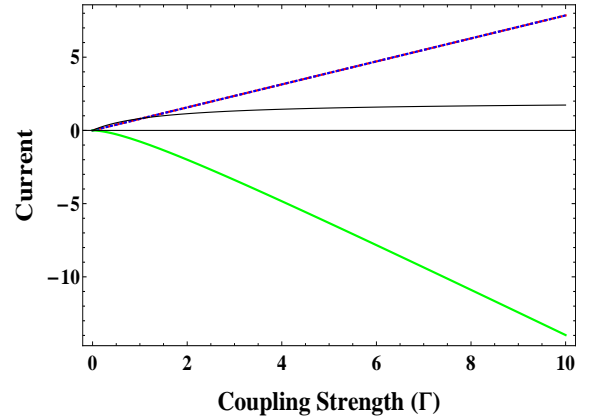


FIG. 4. (Color online) Currents carried by bonding (red-dashed), anti-bonding (blue-dotted) and coherences (green-thick) along with the net current (black-thin) as a function of Γ with $t = 1$, $\beta_L^{-1} = \beta_R^{-1} = 0$, $\mu_L = 1$ and $\mu_R = -1$.

For $\Gamma \gg t$, the current contributions, I_b and I_c , acquire the simple form,

$$I_b = \frac{\Gamma}{2} \left[\tan^{-1} \left(\frac{\Gamma V}{2t^2} \right) + \tan^{-1} \left(\frac{V}{2\Gamma} \right) \right] \\ I_c = \Gamma \left[\tan^{-1} \left(\frac{V}{2\Gamma} \right) - \tan^{-1} \left(\frac{\Gamma V}{2t^2} \right) \right]. \quad (22)$$

Unlike the serially coupled case, in this case both contributions, population as well as the coherences, grow linearly with Γ . However, their sum, the total current, saturates to the value $\Gamma \tan^{-1}(V/2\Gamma)$. We again notice that contributions from the bonding and the anti-bonding

states are always positive while the coherent contribution is always negative for large Γ . This is shown in Fig. (4). It is to be noted that although current through the population and coherence channels increases linearly with Γ , the zero-bias conductivity is quadratic while the finite-bias conductivity reaches a constant value $\pm(t/V)^2$ for the population (+) and coherence (−) channels, respectively.

IV. CONCLUSION

In this work we have explored the effects of system-reservoir coupling on currents through molecular (quantum dot) junctions. It is shown that the net current in a molecular junction is not always a monotonically increasing function of the coupling strength. We have demonstrated this by considering two simple model junctions which are easily realizable in experiments. For a serially arranged double quantum dot system, the net current behaves non-monotonically and goes to zero for large Γ , while for a side-coupled quantum dot system, the current increases monotonically and saturates to a finite non-zero value. These two different current behaviors originate due to competition between the classical and the quantum contributions to the junction conductance. The classical current, described in terms of the eigenstate populations, and the quantum contribution, that comes from the superposition between the eigenstates, have opposite contributions to the net current. The classical part is always positive (flows along the applied bias) while the quantum contribution is always negative for large couplings. For a serially coupled system, for large couplings (Γ), the classical and the quantum contribu-

tions saturate to the same finite value that corresponds to the (quantum) conductivity of a perfect channel. The two contributions therefore tend to cancel each other out completely at large Γ , leading to the net zero current through the junction. On the other hand, for a side-coupled system, the two contributions grow linearly with Γ in opposite directions with the same rate. This results in the net current saturating to a finite value. The coherent contribution in this case is negative for all Γ values.

It is to be noted that while for serially coupled system, the coherent contribution can be positive or negative or even vanish depending on the system parameters, for a side-coupled system, however, the coherent contribution is always negative and is zero only when the net current vanishes. That is for a side-coupled system, the coherent channel always conducts in the direction opposite to the applied bias and can not be blocked to maximize the net current, which is possible for a serially coupled system.

Although the conclusions drawn above are based on calculations on simple model systems, we find that the qualitative results remain valid even for more complicated junctions within more realistic couplings (without wide-band approximation). For example, for a Lorentzian bath spectral density, the results for large couplings ($\Gamma > 2t$) remain valid for both model systems. Similarly, for a circular molecular junction, for example Benzene molecular junction, the population and coherences contribute oppositely to the net current. This seems to be a general trend for currents in molecular junctions.

ACKNOWLEDGEMENTS

H. Y. and U. H. acknowledge the financial support from the Indian Institute of Science, Bangalore, India.

-
- [1] M. Esposito, U. Harbola, and S. Mukamel, Rev. Mod. Phys. **81**, 1665 (2009).
 - [2] Y. Utsumi, D. Golubev, M. Marthaler, K. Saito, T. Fujisawa, and G. Schön, Physical Review B **81**, 125331 (2010).
 - [3] A. Aviram and M. A. Ratner, Chemical Physics Letters **29**, 277 (1974).
 - [4] D. M. Cardamone, C. A. Stafford, and S. Mazumdar, Nano letters **6**, 2422 (2006).
 - [5] M. O. Scully, M. S. Zubairy, G. S. Agarwal, and H. Walther, Science **299**, 862 (2003).
 - [6] H. P. Goswami and U. Harbola, Physical Review A **88**, 013842 (2013).
 - [7] D. Loss and D. P. DiVincenzo, Physical Review A **57**, 120 (1998).
 - [8] W. G. Van der Wiel, S. De Franceschi, J. M. Elzerman, T. Fujisawa, S. Tarucha, and L. P. Kouwenhoven, Reviews of Modern Physics **75**, 1 (2002).
 - [9] U. Harbola, M. Esposito, and S. Mukamel, Physical Review B **74**, 235309 (2006).
 - [10] S. Datta, *Electronic transport in mesoscopic systems* (Cambridge university press, 1997).
 - [11] H. Haug and A.-P. Jauho, *Quantum kinetics in transport and optics of semiconductors* (Springer, 1996).
 - [12] W. H. Zurek, Reviews of modern physics **75**, 715 (2003).
 - [13] Y. Meir and N. S. Wingreen, Physical review letters **68**, 2512 (1992).
 - [14] J. Rammer, *Quantum field theory of non-equilibrium states* (Cambridge University Press, 2007).
 - [15] H. K. Yadalam and U. Harbola, Physical Review B **94**, 115424 (2016).